Highly Dispersed γ-Fe_2O_3 Embedded in Nitrogen Doped Carbon for Efficient Oxygen Reduction Reaction

Zhourong Xiao[a], Guoqiang Sheng[a], Fang Hou[a], Rongrong Zhang[a], Yueting Li[a], Gang Yuan[a], Lun Pan[a,b], JiJun Zou[a,b], Li Wang[a,b], Xiangwen Zhang[a,b], Guozhu Li[a,b]*

[a] Key Laboratory for Green Chemical Technology of Ministry of Education, School of Chemical Engineering and Technology, Tianjin University, Tianjin 300072, China

[b] Collaborative Innovation Center of Chemical Science and Engineering (Tianjin), Tianjin 300072, China

*Corresponding author. Tel. /fax: +86 22 27892340.

E-mail address:

1. Experiment

1.1 Catalyst preparation

The catalyst fabrication procedure is described in Scheme 1. 1.20 g of $FeCl_3 \cdot 6H_2O$, 1.00 g of glycine and 2 g of MgO nanoparticles (50 nm, Nanjing XianFeng Nano) were mixed in 5 mL water and sonicated for 15 min, followed by vigorously stirred for 6 h. Then the mixture was dried at 70 ^oC for 24 h, and then grinded and transferred to a quartz boat in the oven. The sample was fluxed with N_2 (50 ml/min) at different carbonization temperature (600 ^oC, 700 ^oC, 800 ^oC, 900 ^oC) for 2 h. The obtained black solid was added in 50 ml HNO_3 solution (1 mol/L) and stirred at room temperature for 30 min. The above leaching procedure was repeated for 2 times to completely remove the MgO template. The recovered black solid was washed with ethanol and water until the filtrate became neutral, and then the sample was dried at 60 ^oC for 24 h. The resultant sample is labeled as Fe_2O_3@NC-T (T = carbonization temperature). For comparison, sample without the addition of $FeCl_3 \cdot 6H_2O$ was synthesized at carbonization temperature of 800 ^oC by similar procedure and named as NC. Moreover, a series of catalysts with the addition of different amounts of $FeCl_3 \cdot 6H_2O$ (0.2 g, 0.4 g, 0.8 g, 1.6 g) were also prepared at the carbonization temperature of 800 ^oC and named as Fe_2O_3@NC-x (x = 0.2, 0.4, 0.8, 1.6). The pure γ-Fe_2O_3 was purchased from Sigma.

1.2. Characterization

Surface area and pore structure of the catalysts were characterized by N_2 adsorption-desorption at -196 ^oC using a Micromeritics Tristar 3000 analyzer. Pore distribution and the cumulative volume of pores were obtained by the Barret-Joyner-Halenda (BJH) method from the desorption branches of the N_2 isotherms. XRD was performed on a Rigaku D8-Focus diffractometer employing the graphite filtered Cu *K*α radiation

(λ = 1.54056 Å). Scanning electron microscopy (SEM) used in this paper is a FEI Nanosem 430. Raman spectra of the as-prepared catalysts were measured on a DXR Microscope system. 50 mg of the sample was excited using an argon laser operating at 532 nm for the Raman test. For the Raman shift from 200 cm^{-1} to 800 cm^{-1}, argon laser operating at 633 nm was adopted. Transmission electron microscopy (TEM) and high-resolution TEM (HR-TEM) images were collected using a Tecnai G2 F-20 microscope. The TEM samples were prepared by dropping and drying the solution of sample on holey carbon coated Cu grids. Electron energy loss spectroscopy (EELS) mapping analysis was carried out on Titan G2 60-300 Probe Cs Corrector UHRSTEM. X-ray absorption fine structure spectroscopy (XAFS) was performed at the 1W2B beamline, Beijing Synchrotron Radiation Facility. During the experiments, the storage ring with 2.5 GeV electrons at 250 mA constantly was used. X-ray photoelectron spectra (XPS) were recorded on an ESCALAB 250Xi spectrometer (Thermo Fisher Scientific) with an Al *Kα* (hν = 1486.6 eV) X-ray source. ^{57}Fe-Mössbauer spectra were recorded at room temperature by means of a conventional constant-acceleration spectrometer with γ-ray source of mCi^{57}Co in a palladium matrix.

1.3. Electrode preparation and electrochemical measurements

1.3.1. Working electrode preparation

A mirror-like surface of the glassy carbon electrode (GCE, 5 mm in diameter, geometric area = 0.196 cm^2) was obtained by polishing with 1 μm, 0.5 μm and 0.05 μm alumina powder slurry, respectively, and then ultrasonicating several times in ethanol and deionized water. A mixture containing of the as-prepared catalyst (3 mg), 1 ml water-isopropyl alcohol solution was firstly prepared. The obtained solution was ultrasonicated for 30 min. Then, 25 μL Nafion solution was added to the mixture followed by ultrasonication for at least 2 h. Finally, 15 μL of the homogeneous ink

was coated on the surface of GCE, which was dried under room temperature for 4 h to form a catalyst film. 0.229 mg cm^{-2} of the catalyst was loaded on GCE. Similar process was adopted to load 20 wt% Pt/C on GCE with a loading amount of 0.229 mg cm^{-2}.

1.3.2. Electrochemical measurement

CompactStat.h10800 potentiostat/galvanostat/elctrochemical analyser (Ivium Technologies Co., Netherland), combining with a rotation speed controller (Pine Instrument Co., USA), was employed to perform the electrochemical measurement. A three-electrode system was set up and used for elctrochemical data collection. RHE was used as the reference electrode, a graphite rod was selected as the counter electrode, and the catalyst-coated GCE was served as the working electrode, respectively.

Cyclic voltammetry (CV) curves were collected in O_2-saturated or Ar-saturated KOH solution (0.1 M) at a scan rate of 50 mV s^{-1} from 0.164 V to 1.164 V (vs RHE, the potential is relative to RHE unless specifically illustrated hereinafter). The polarization plots for ORR (linear sweep voltammetry, LSV) were obtained using the rotating disk electrode (RDE) technique in O_2-saturated KOH solution (0.1 M). Commercial Pt/C (20 wt%) was obtained from HeSen Electric Co., and used as the benchmark.

The number of electrons transferred per O_2 molecule (n) in ORR was calculated using Koutecky-Levich (K-L) equation listed below.

$$\frac{1}{J} = \frac{1}{J_L} + \frac{1}{J_K} = \frac{1}{B\omega^{1/2}} + \frac{1}{nFkC_0}$$

$$B = 0.2nFC_0D_0^{2/3}\nu^{-1/6}$$

Where J_L is the limiting diffusion current density (mA cm^{-2}), J is the measured

current density (mA cm^{-2}), F is the Faraday constant (96485 C mol^{-1}), ω is the rotating speed (rpm), C_0 is the bulk concentration of O_2 (1.2×10^{-6} mol cm^{-3}), ν is the kinetic viscosity of the electrolyte (0.01 cm^2 s^{-1}), k is the electron-transfer rate constant, and D_0 is the O_2 diffusion coefficient (1.9×10^{-5} cm^2 s^{-1}).

The electron transfer number (n) was verified based on ring current (I_{ring}) and disk current (I_{disk}) by RRDE measurement at 1600 rpm. Where N, representing the collection efficiency of Pt ring, equals to 0.37.

$$n = 4 \times \frac{I_{disk}}{(I_{disk} + I_{ring}/N)}$$

1.3.3. Zinc-air battery measurement

To further investigation the real application of the as synthesized catalyst, the primary zinc-air battery was constructed using a polished zinc plate as the anode. The catalyst prepared by our or 20 wt% Pt/C catalyst electrode as the air cathode. The air cathode was prepared by spraying the catalyst onto carbon paper, and then dried at room temperature for 4 h. These two electrodes and 6 M KOH aqueous electrolyte were assembled into a home-made zinc-air battery. The catalyst mass loading was 0.667 mg cm^{-2}.

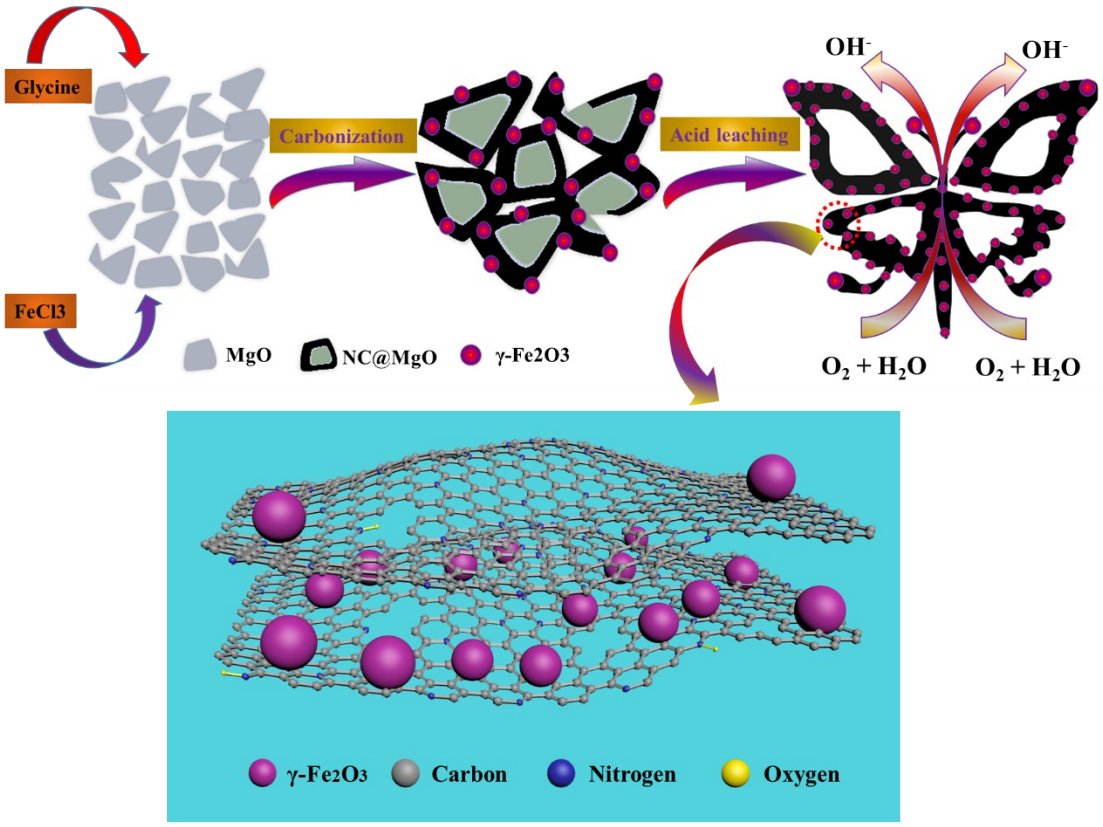

Scheme 1. Illustration of catalyst preparation.

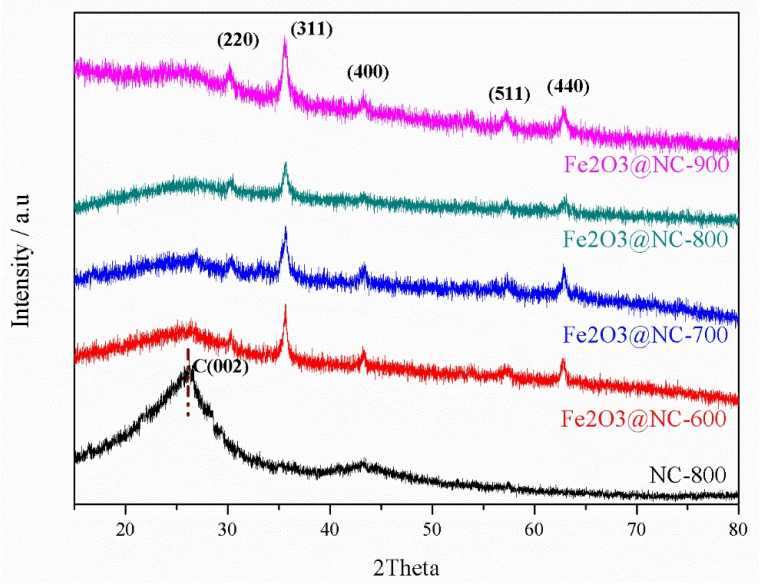

Fig. S1 XRD patterns of the as-prepared catalysts.

Table S1 - Mössbauer parameters of Fe_2O_3@NC-800 derived from the fittings. Isomer shift (IS), line width (LW) and relative spectral area % of each component.

Type	δ_{iso}/mm s^{-1}	LW/mm s-1	Area (%)
Sextet peaks	0.39	1.61	39.3
Doublet 1	0.36	0.68	31.5
Doublet 2	0.55	1.01	29.2

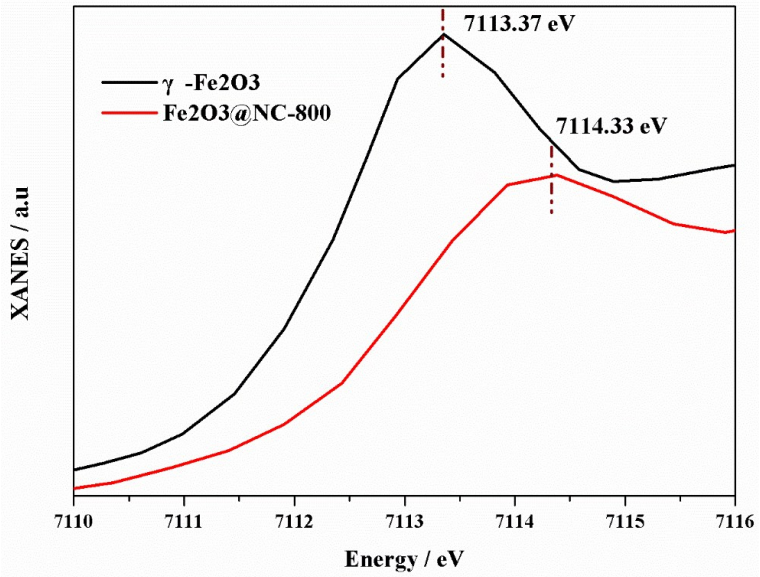

Fig. S2 Fe K-edge XANES spectra.

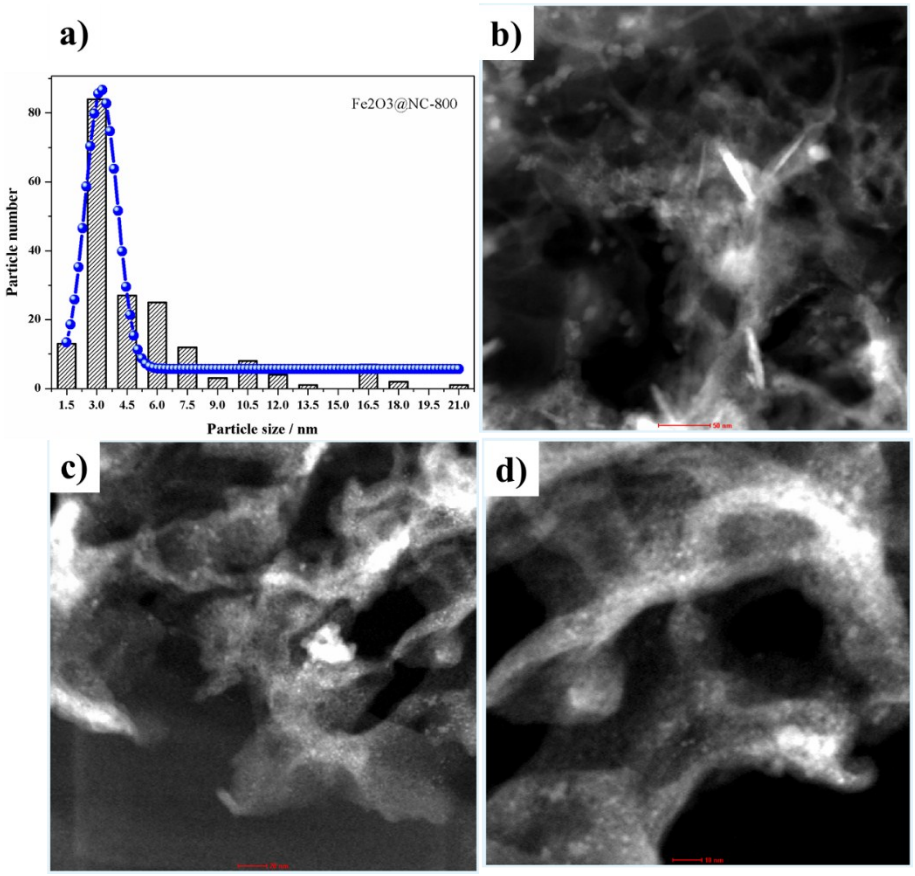

Fig. S3 (a) Particle size distribution of γ-Fe_2O_3 for Fe_2O_3@NC-800, (b-d) corresponding TEM images for the count of particles size.

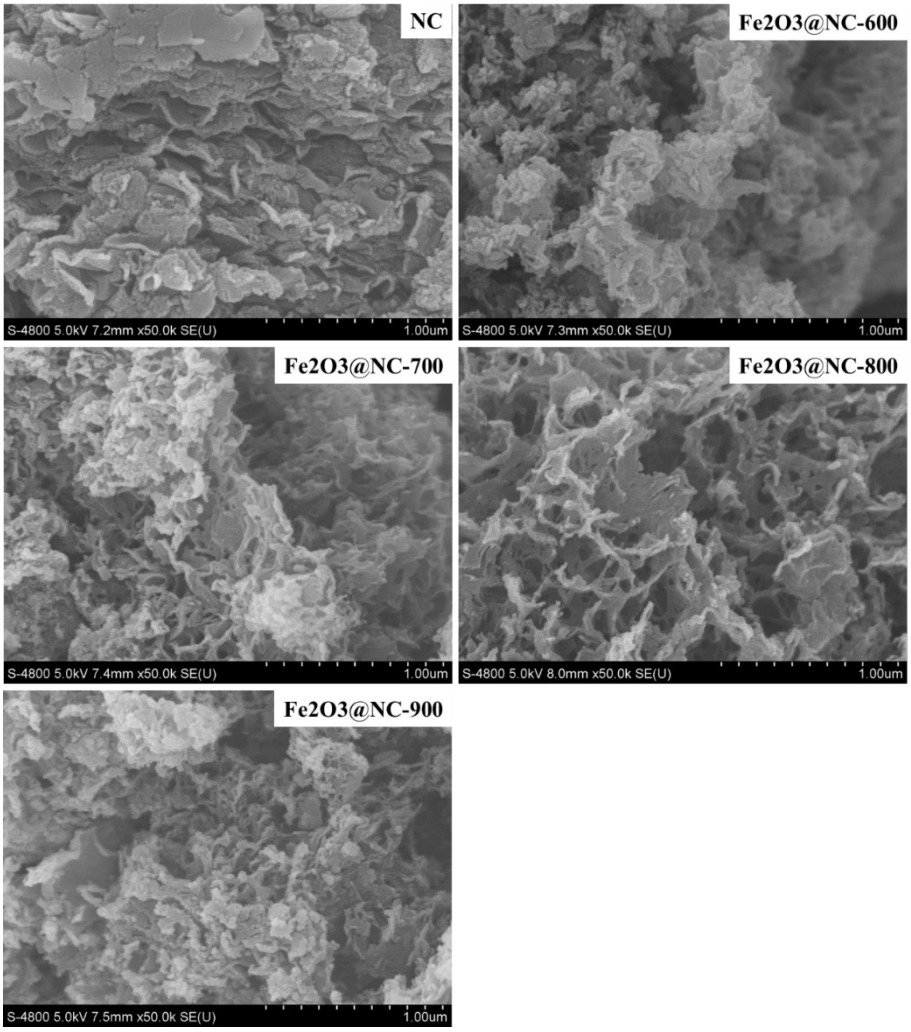

Fig. S4 SEM images of as-prepared samples.

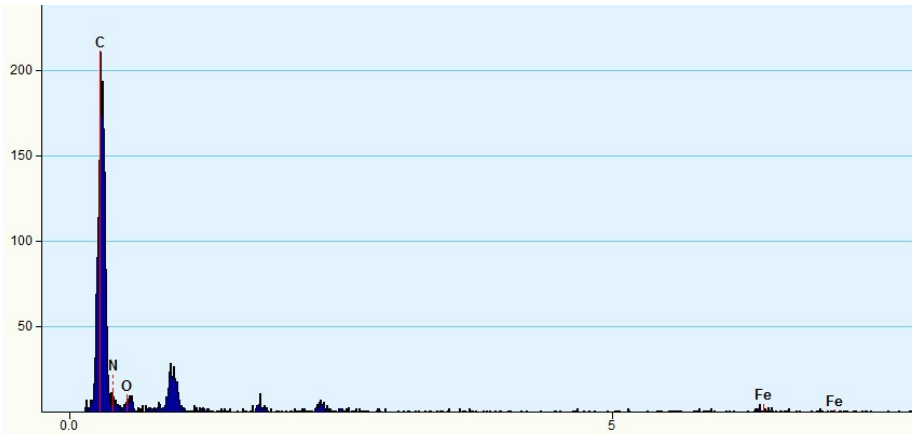

Fig. S5 EDX analysis of Fe_2O_3@NC-800.

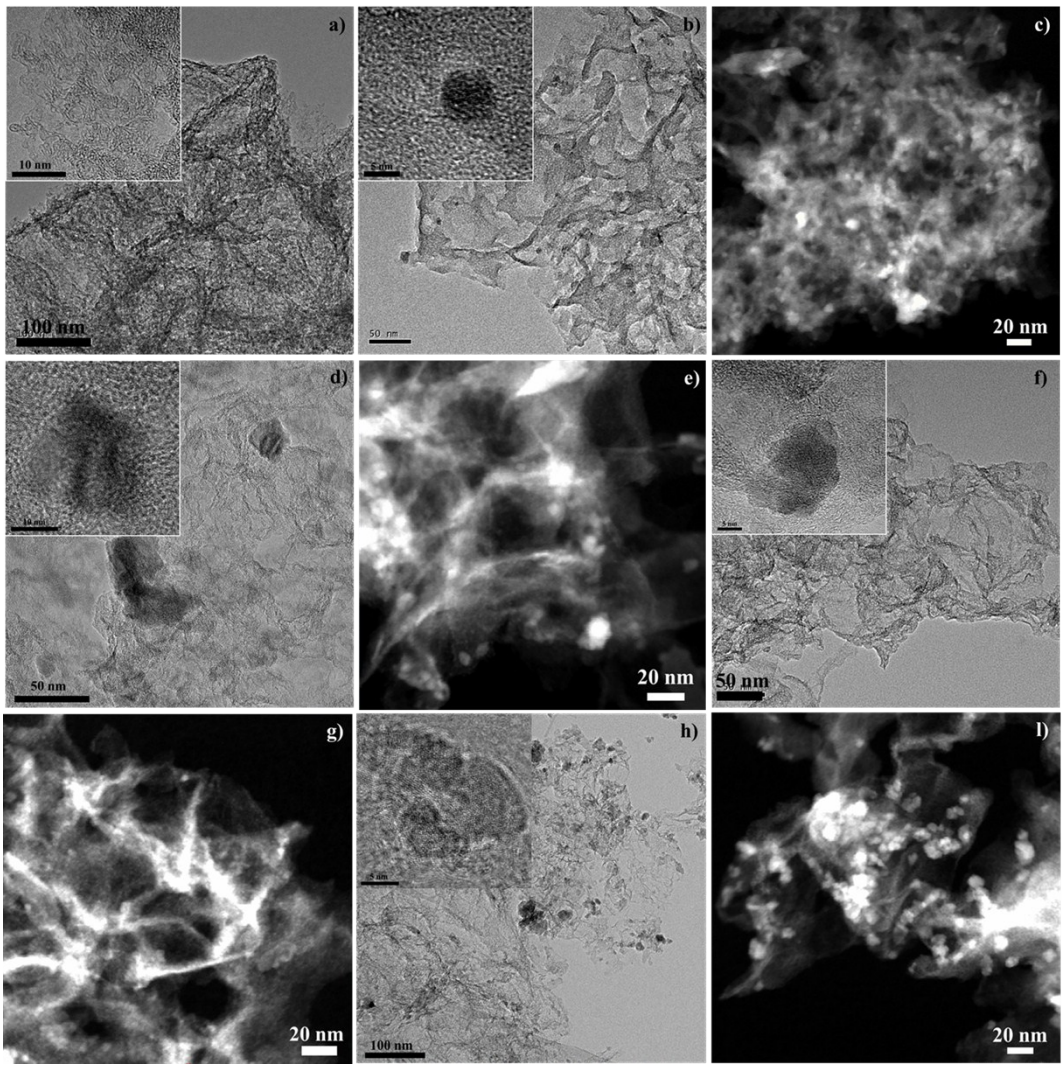

Fig. S6 TEM images of as-prepared samples. (a) NC, (b-c) Fe_2O_3@NC-600, (d-e) Fe_2O_3@NC-700, (f-g) Fe_2O_3@NC-800, (h-i) Fe_2O_3@NC-900.

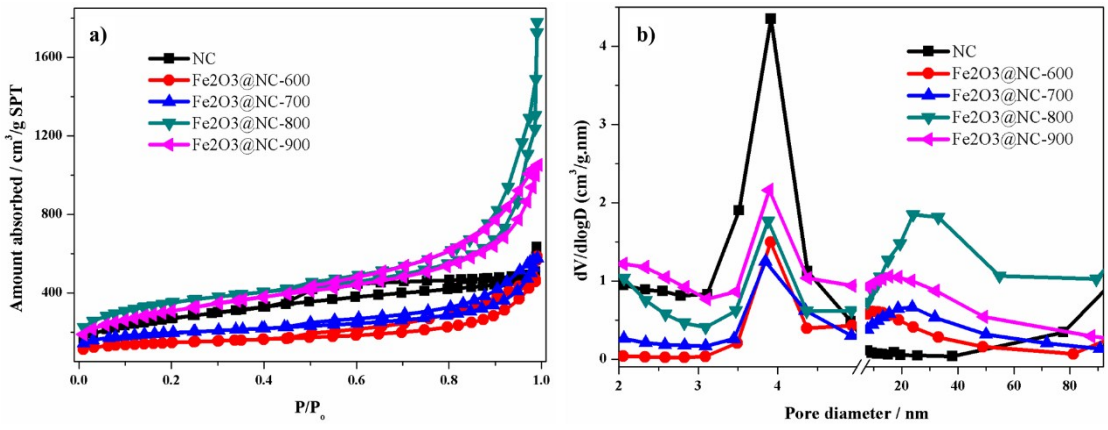

Fig. S7 (a) Nitrogen adsorption-desorption isotherm and (b) pore size distribution of as-prepared samples.

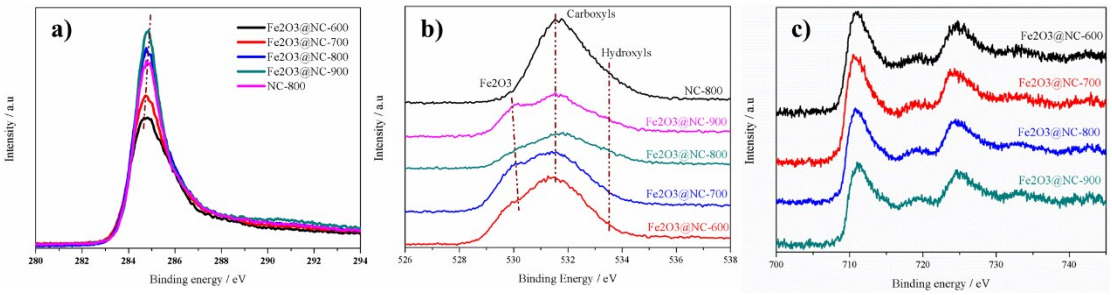

Fig. S8 XPS spectra of as-prepared samples, (a) C 1s, (b) O 1s, (c) Fe 2p.

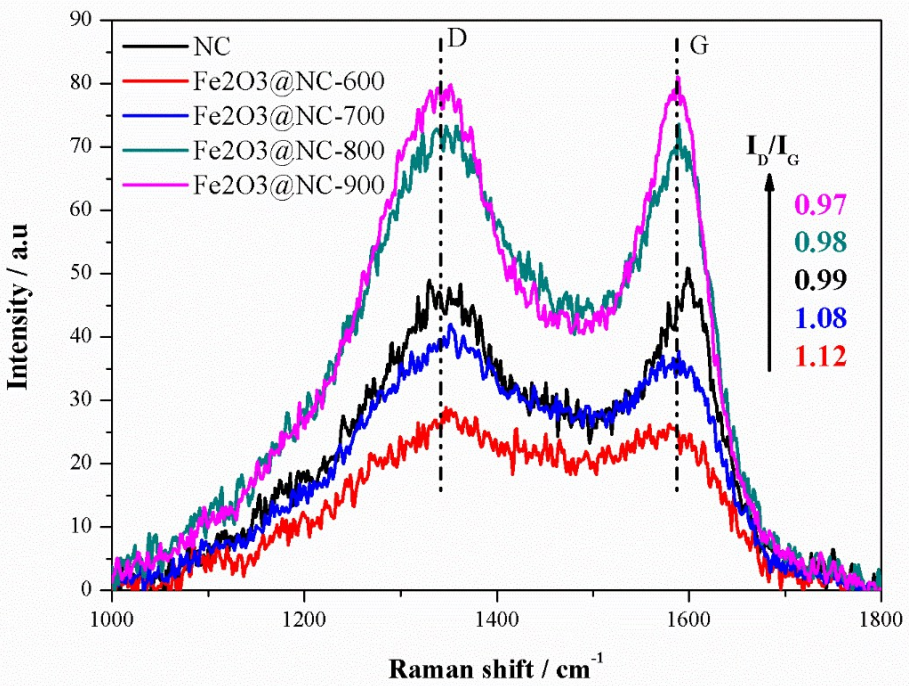

Fig. S9 Raman spectra of as-prepared sample.

Table S2 - Surface compositions of the as-prepared catalysts.

Element	NC	Fe_2O_3@NC-600	Fe_2O_3@NC-700	Fe_2O_3@NC-800	Fe_2O_3@NC-900
C 1s	76.13	64.91	68.95	77.20	81.85
N 1s	5.89	14.35	11.38	5.69	3.61
O 1s	17.70	17.23	16.16	13.87	11.58
Fe 2p	0.28	3.51	3.51	3.24	2.97

Table S3 - The ratio of different type of N element.

Element	NC	Fe_2O_3@ NC-600	Fe_2O_3@ NC-700	Fe_2O_3@ NC-800	Fe_2O_3@ NC-900
Pyridinic N	26.58	42.31	34.47	21.52	14.26
Pyrrolic N	10.31	17.13	17.45	16.65	18.22
Graphitic N	45.69	28.82	37.66	50.16	50.04
Oxidized N	17.42	11.74	10.41	11.68	17.49

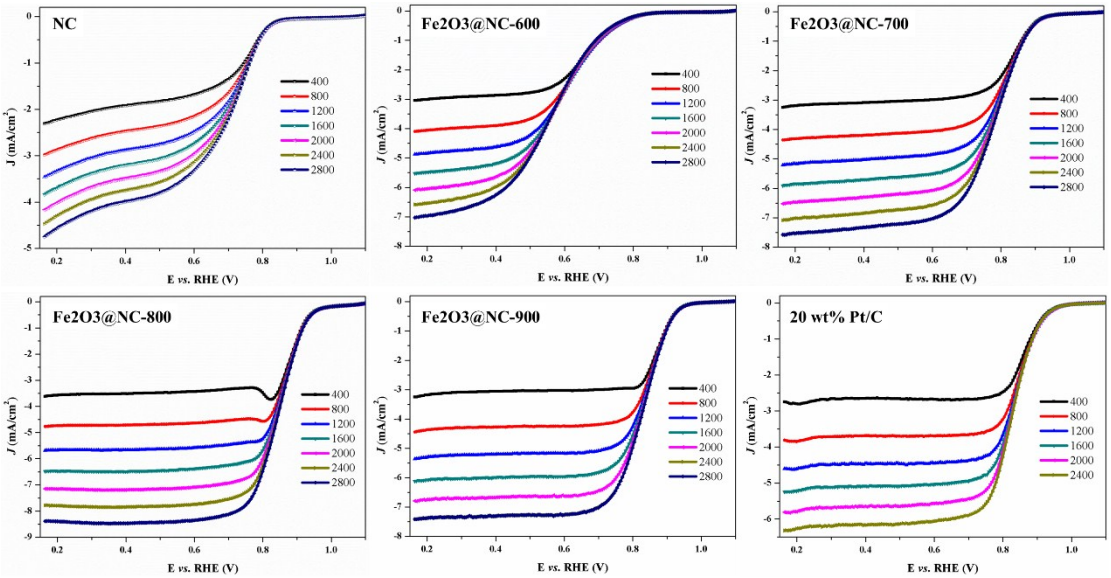

Fig. S10 Linear sweep voltammograms recorded in O_2-saturated 0.1 M KOH at a scan rate of 10 mV s^{-1}.

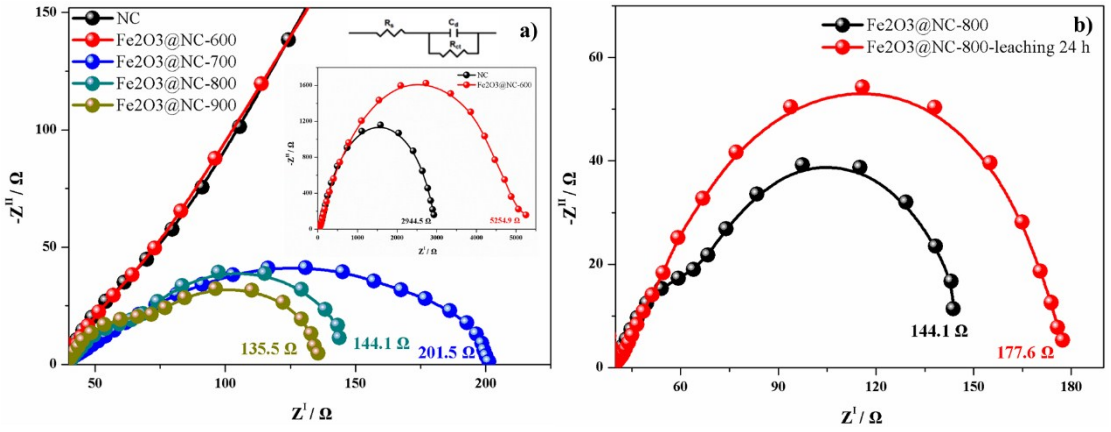

Fig. S11 Electrochemical impedance spectra.

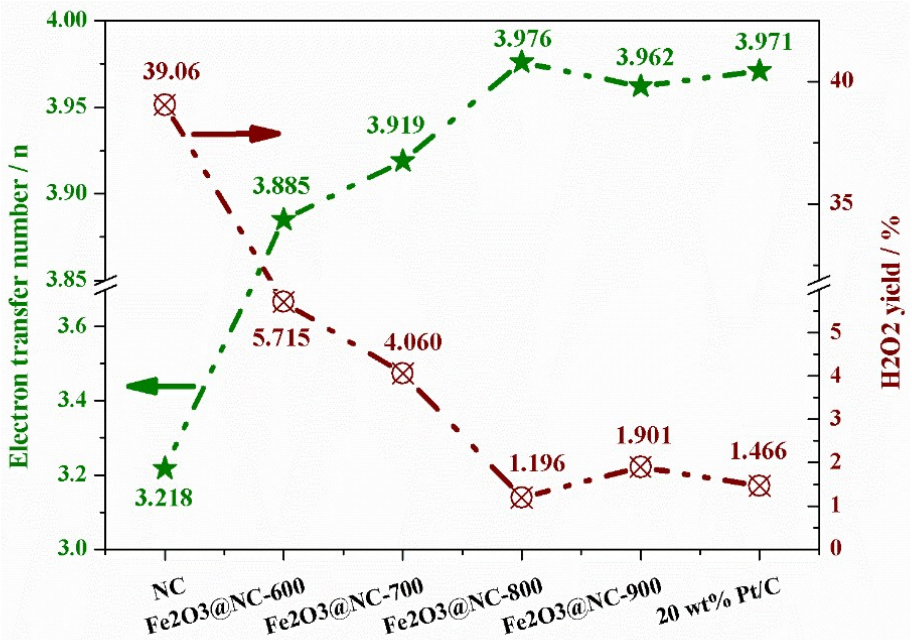

Fig. S12 Electron transfer numbers and H_2O_2 yields (0.464 V. RHE) on various catalysts.

Table S4 - Comparison of ORR performance between Fe_2O_3@NC-800 and those reported previously in other's works.

Catalysts	Loading (mg cm^{-2})	$\Delta E_{1/2}$(RHE, mV)[a]	J_L (mA cm^{-2}) （RHE）	Refs.
α-Fe_2O_3/CNTs	0.204	-120	1.31 (0.364 V)	1
OMCs-Fe_2O_3	0.500	-30	3.91 (0.364 V)	2
ND-Fe_3O_4	0.100	-111	5.25 (0.504 V)	3
Fe-Fe_2O_3/RGO	0.255	-45	6.31 (0.454 V)	4
Fe-Fe_2O_3@NC	0.240	-50	4.00 (0.244 V)	5
Fe-N-C/CNTs-800	0.229	-130	4.50 (0.364 V)	6
Fe-PDA-C	0.500	-120	2.30 (0.464 V)	7
α-Fe_2O_3/ Fe_3O_4/NC	0.120	7	6.02 (0.464 V)	8
Fe/NMC-11	0.510	7	6.12 (0.464 V)	9
Fe@C-FeNCs-2	0.626	5	5.35 (0.464 V)	10
Fe,N-OMC	0.080	12	4.13 (0.464 V)	11

Fe/Fe_3C@N-rGO	0.150	0	5.15 (0.464 V)	12
Fe-ANCS-3	0.495	6	6.00 (0.464 V)	13
MZ8-S-P	0.400	28	5.35 (0.464 V)	14
FeN_2/NOMC-3	0.500	33	4.98 (0.464 V)	15
Fe_3O_4/N-C-900	0.150	-21	5.12 (0.364 V)	16
Fe_3O_4/N-MCS-2	0.318	24	5.51 (0.464 V)	17
Fe-N/MCN	0.196	30	5.20 (0.464 V)	18
Fe_2O_3@NC-800	0.229	28	6.49 (0.464 V)	This work

a: $\Delta E_{1/2} = E_{1/2}(Fe_2O_3@NC\text{-}800) - E_{1/2}(20\ wt\%\ Pt/C)$. The electrolyte is 0.1 M KOH.

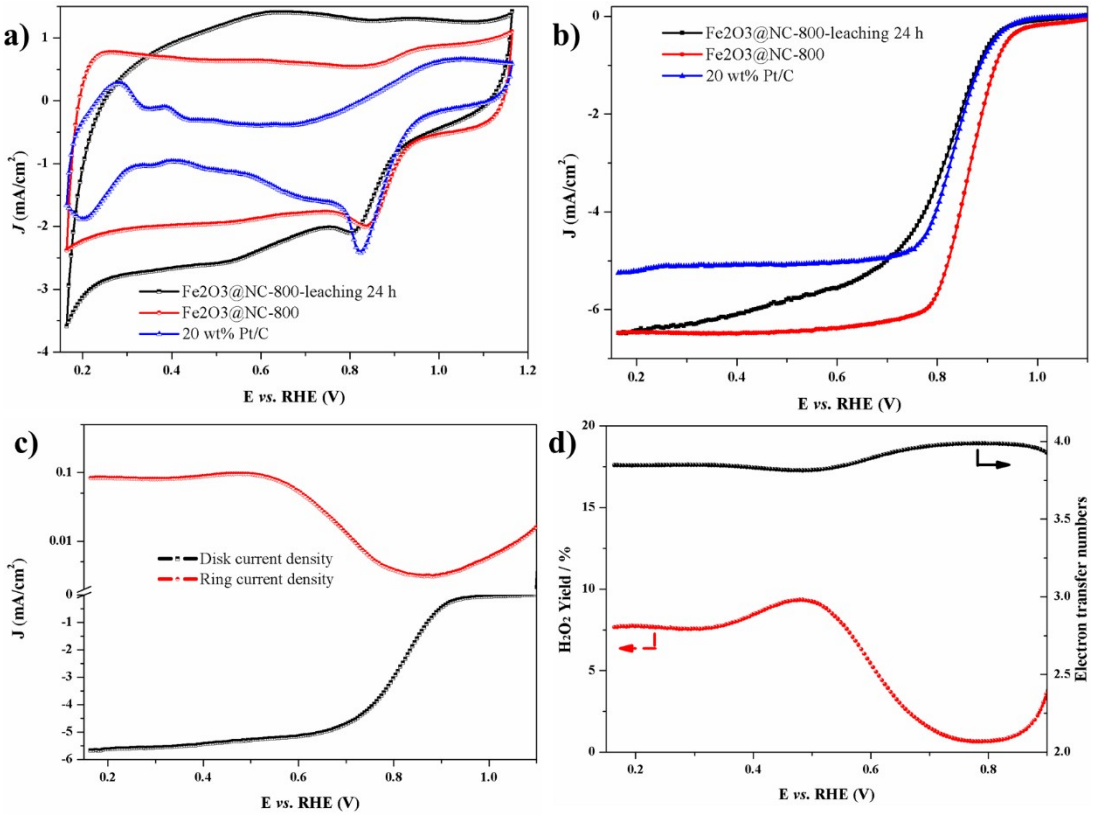

Fig. S13 (a) Cyclic voltammograms of Fe_2O_3@NC-800 leaching for 24 h vs. RHE in 0.1 M KOH (O_2-saturated), (b) Linear sweep voltammograms recorded in O_2-saturated 0.1 M KOH at a scan rate of 10 mV s^{-1} and rotation speed of 1600 rpm, (c) RRED of ring current and RRED of disk current, (d) H_2O_2 yield and Electron transfer numbers (the disk was set to scan at 5 mV s^{-1} from 1.2 V to 0.16 V and the ring was set at 0.3 V)

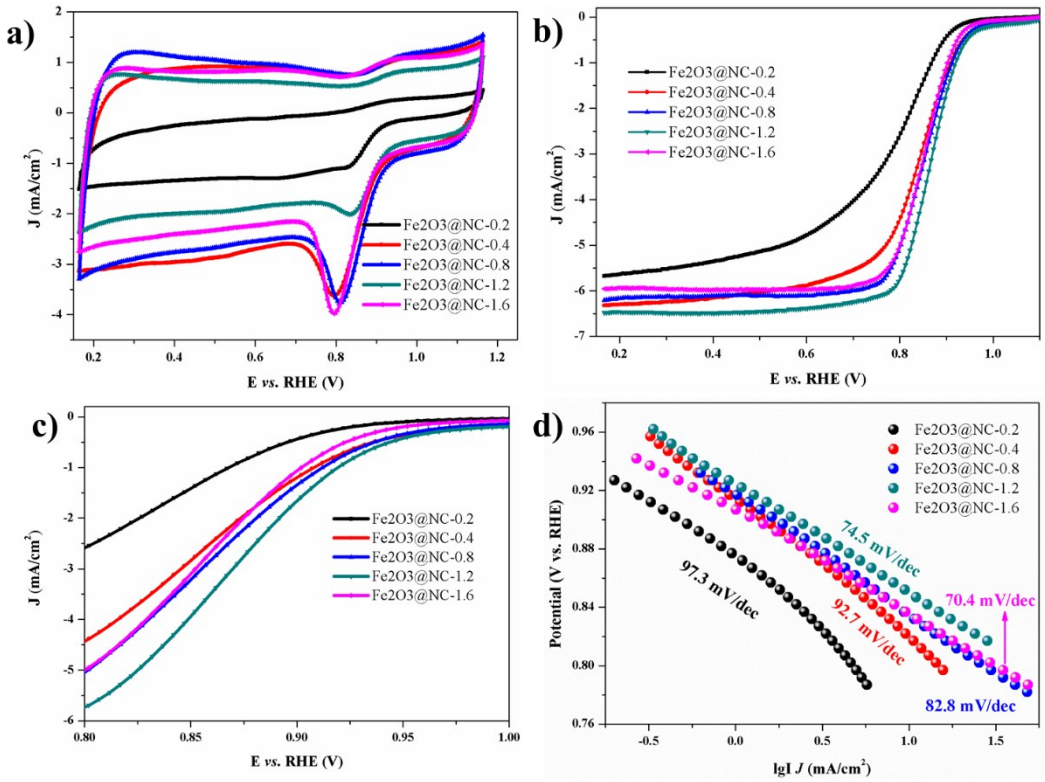

Fig. S14 Cyclic voltammograms of as-prepared samples and 20 wt% Pt/C vs. RHE in 0.1 M KOH (O_2-saturated), (b) Linear sweep voltammograms recorded in O_2-saturated 0.1 M KOH at a scan rate of 10 mV s^{-1} and rotation speed of 1600 rpm, (c) Enlargement of LSV at the voltage of 0.764 V to 1.0 V, (d) ORR Tafel slope.

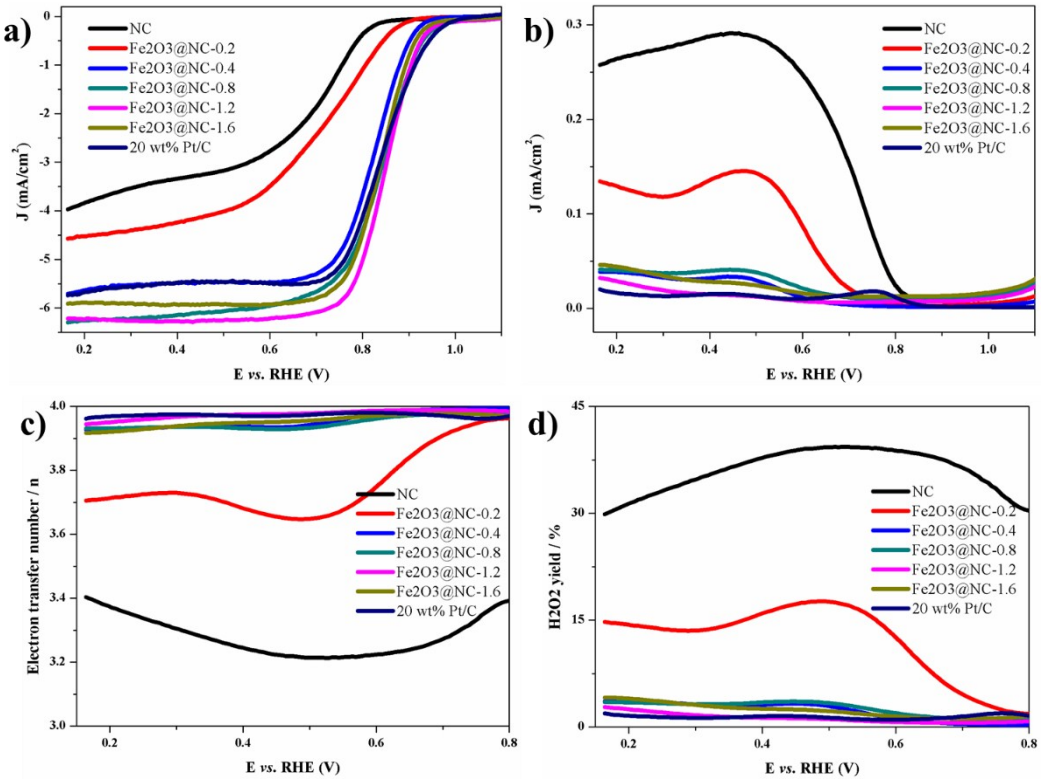

Fig. S15 (a) RRED of ring current, (b) RRED of disk current, (c) H_2O_2 yield, (d) electron transfer numbers (the disk was set to scan at 5 mV s^{-1} from 0.15 V to 1.1 V and the ring was set at 0.3 V) of the as-prepared catalysts

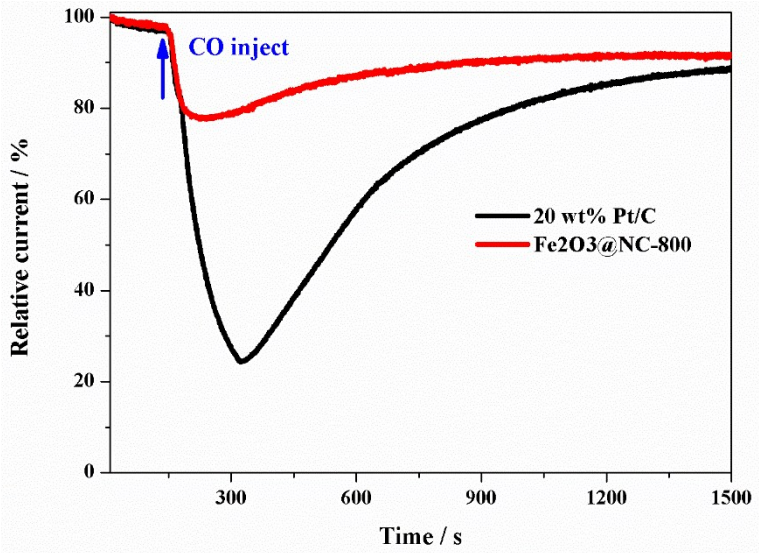

Fig. S16 The abilities of tolerance against CO for different catalysts.

References

[1] M. Sun, Y. Dong, G. Zhang, J. Qu, J. Li, α-Fe_2O_3 spherical nanocrystals supported on CNTs as

efficient non-noble electrocatalysts for the oxygen reduction reaction, Journal of Materials Chemistry A, 2 (2014) 13635-13640.

[2] J. He, B. Li, J. Mao, Y. Liang, X. Yang, Z. Cui, S. Zhu, Z. Li, Four-electron oxygen reduction from mesoporous carbon modified with Fe_2O_3 nanocrystals, Journal of Materials Science, 52 (2017) 10938-10947.

[3] L. Hadidi, E. Davari, D.G. Ivey, J.G. Veinot, Microwave-assisted synthesis and prototype oxygen reduction electrocatalyst application of N-doped carbon-coated Fe_3O_4 nanorods, Nanotechnology, 28 (2017) 095707.

[4] V.M. Dhavale, S.K. Singh, A. Nadeema, S.S. Gaikwad, S. Kurungot, Nanocrystalline Fe-Fe_2O_3 particle-deposited N-doped graphene as an activity-modulated Pt-free electrocatalyst for oxygen reduction reaction, Nanoscale, 7 (2015) 20117-20125.

[5] H. Wang, X. Cheng, F. Yin, B. Chen, T. Fan, X. He, Metal-organic gel-derived Fe-Fe_2O_3@nitrogen-doped-carbon nanoparticles anchored on nitrogen-doped carbon nanotubes as a highly effective catalyst for oxygen reduction reaction, Electrochimica Acta, 232 (2017) 114-122.

[6] Y. Gao, L. Wang, G. Li, Z. Xiao, Q. Wang, X. Zhang, Taming transition metals on N-doped CNTs by a one-pot method for efficient oxygen reduction reaction, International Journal of Hydrogen Energy, 43 (2018) 7893-7902.

[7] B. Li, Y. Chen, X. Ge, J. Chai, X. Zhang, T.S.A. Hor, G. Du, Z. Liu, H. Zhang, Y. Zong, Mussel-inspired one-pot synthesis of transition metal and nitrogen co-doped carbon (M/N-C) as efficient oxygen catalysts for Zn-air batteries, Nanoscale, 8 (2016) 5067-5075.

[8] H. Fan, K. Mao, M. Liu, O. Zhuo, J. Zhao, T. Sun, Y. Jiang, X. Du, X. Zhang, Q. Wu, R. Che, L. Yang, Q. Wu, X. Wang, Z. Hu, Tailoring the nano heterointerface of hematite/magnetite on hierarchical nitrogen-doped carbon nanocages for superb oxygen reduction, Journal of Materials Chemistry A, 6 (2018) 21313-21319.

[9] L. Zhuang, S. Fei, G. Lin, G. Chen, T. Shang, L. Jing, Z. Le, X. Li, B.W. Hao, Y. Lu, Post Iron Decoration of Mesoporous Nitrogen-Doped Carbon Spheres for Efficient Electrochemical Oxygen Reduction, Advanced Energy Materials, 7 (2017) 1701154.

[10] M. Hoque, S. Zhang, M.L. Thomas, Z. Li, S. Suzuki, A. Ando, M. Yanagi, Y. Kobayashi, K. Dokko, M. Watanabe, Simple combination of a protic salt and an iron halide: precursor for a Fe, N and S co-doped catalyst for the oxygen reduction reaction in alkaline and acidic media, Journal of

Materials Chemistry A, 6 (2018) 1138-1149.

[11] X. Liu, S. Zou, S. Chen, Ordered mesoporous carbons codoped with nitrogen and iron as effective catalysts for oxygen reduction reaction, Nanoscale, 8 (2016) 19249-19255.

[12] Y. Liu, H. Wang, D. Lin, J. Zhao, C. Liu, J. Xie, Y. Cui, A Prussian blue route to nitrogen-doped graphene aerogels as efficient electrocatalysts for oxygen reduction with enhanced active site accessibility, Nano Research, 10 (2016) 1213-1222.

[13] R. Ma, Y. Zhou, C. Hu, M. Yang, F. Wang, K. Yan, Q. Liu, J. Wang, Post iron-doping of activated nitrogen-doped carbon spheres as a high-activity oxygen reduction electrocatalyst, Energy Storage Materials, 13 (2018) 142-150.

[14] Y. Qian, T. An, K.E. Birgersson, Z. Liu, D. Zhao, Web-Like Interconnected Carbon Networks from NaCl-Assisted Pyrolysis of ZIF-8 for Highly Efficient Oxygen Reduction Catalysis, Small, 14 (2018) 1704169.

[15] H. Shen, E. Gracia-Espino, J. Ma, H. Tang, X. Mamat, T. Wagberg, G. Hu, S. Guo, Atomically FeN2 moieties dispersed on mesoporous carbon: A new atomic catalyst for efficient oxygen reduction catalysis, Nano Energy, 35 (2017) 9-16.

[16] Y. Su, H. Jiang, Y. Zhu, X. Yang, J. Shen, W. Zou, J. Chen, C. Li, Enriched graphitic N-doped carbon-supported Fe_3O_4 nanoparticles as efficient electrocatalysts for oxygen reduction reaction, J. Mater. Chem. A, 2 (2014) 7281-7287.

[17] H. Wang, W. Wang, M. Gui, M. Asif, Z. Wang, Y. Yu, J. Xiao, H. Liu, Uniform Fe3O4/Nitrogen-Doped Mesoporous Carbon Spheres Derived from Ferric Citrate-Bonded Melamine Resin as an Efficient Synergistic Catalyst for Oxygen Reduction, ACS applied materials & interfaces, 9 (2017) 335-344.

[18] W. Jing, L. Yan, Z. Xinyi, G.P. Simon, Z. Dongyuan, Z. Jin, J. Sanping, W. Huanting, Controllable synthesis of mesoporous carbon nanospheres and Fe-N/carbon nanospheres as efficient oxygen reduction electrocatalysts, Nanoscale, 7 (2015) 6247-6254.